Neurophotonics

Neurophotonics.SPIEDigitalLibrary.org

Ryanodine and IP_3 receptor-mediated calcium signaling play a pivotal role in neurological infrared laser modulation

Gleb P. Tolstykh
Cory A. Olsovsky
Bennett L. Ibey
Hope T. Beier

SPIE.

Gleb P. Tolstykh, Cory A. Olsovsky, Bennett L. Ibey, Hope T. Beier, "Ryanodine and IP_3 receptor-mediated calcium signaling play a pivotal role in neurological infrared laser modulation," *Neurophoton.* **4**(2), 025001 (2017), doi: 10.1117/1.NPh.4.2.025001.

Neurophotonics 4(2), 025001 (Apr–Jun 2017)

Ryanodine and IP_3 receptor-mediated calcium signaling play a pivotal role in neurological infrared laser modulation

Gleb P. Tolstykh,[a,*] Cory A. Olsovsky,[b] Bennett L. Ibey,[c] and Hope T. Beier[d]
[a]General Dynamics Information Technology, JBSA Fort Sam Houston, San Antonio, Texas, United States
[b]Texas A&M University, Department of Biomedical Engineering, College Station, Texas, United States
[c]Air Force Research Laboratory, 711th Human Performance Wing, Airman Systems Directorate, Bioeffects Division, Radio Frequency Bioeffects Branch, JBSA Fort Sam Houston, San Antonio, Texas, United States
[d]Air Force Research Laboratory, 711th Human Performance Wing, Airman System Directorate, Bioeffects Division, Optical Radiation Bioeffects Branch, JBSA Fort Sam Houston, San Antonio, Texas, United States

Abstract. Pulsed infrared (IR) laser energy has been shown to modulate neurological activity through both stimulation and inhibition of action potentials. While the mechanism(s) behind this phenomenon is (are) not completely understood, certain hypotheses suggest that the rise in temperature from IR exposure could activate temperature- or pressure-sensitive ion channels or create pores in the cellular outer membrane, allowing an influx of typically plasma-membrane-impermeant ions. Studies using fluorescent intensity-based calcium ion (Ca^{2+}) sensitive dyes show changes in Ca^{2+} levels after various IR stimulation parameters, which suggests that Ca^{2+} may originate from the external solution. However, activation of intracellular signaling pathways has also been demonstrated, indicating a more complex mechanism of increasing intracellular Ca^{2+} concentration. We quantified the Ca^{2+} mobilization in terms of influx from the external solution and efflux from intracellular organelles using Fura-2 and a high-speed ratiometric imaging system that rapidly alternates the dye excitation wavelengths. Using nonexcitable Chinese hamster ovarian (CHO-hM_1) cells and neuroblastoma-glioma (NG108) cells, we demonstrate that intracellular IP_3 receptors play an important role in the IR-induced Ca^{2+}, with the Ca^{2+} response augmented by ryanodine receptors in excitable cells. [DOI: 10.1117/1.NPh.4.2.025001]

Keywords: infrared stimulation; calcium; intracellular signaling; plasma membrane poration; ion channels.

Paper 16069PRR received Dec. 1, 2016; accepted for publication Mar. 20, 2017; published online Apr. 5, 2017.

1 Introduction

Application of infrared (IR) laser pulses with wavelengths ranging from 1.4 to 2.1 μm and pulse durations in the order of micro- to milliseconds has been shown to directly stimulate nerves without any chemical pretreatment or genetic alteration.[1–8] Likewise, ~1.8 μm IR pulse exposure has also been demonstrated to block action potential (AP) generation and propagation.[9–13] While a rapid increase in temperature, due to absorption of the laser radiation, is required to evoke the neural depolarization, and IR stimulation pulses have been shown to produce an acoustic pressure wave,[14–17] the mechanism(s) to stimulate or inhibit an AP is not fully understood.[18] Certain thermal and mechanical mechanisms[17,19] involving ion channels, such as transient receptor potential (TRP) channel activation,[20] plasma membrane poration,[21] and/or membrane potential changes, are suggested as explanations for IR neural stimulation and inhibition, together termed IR neural modulation (INM).[1] Shapiro et al.[22,23] also showed that the rapid temperature change slightly depolarizes the plasma membrane through capacitive charging. This effect could initiate AP firing in neurons but cannot explain IR-induced neuronal inhibition.

While much research into the mechanisms underlying IR stimulation has focused on the interaction of the IR pulse with plasma membrane, the diverse responses to INM suggest the possibility that intracellular physiological regulatory and compensatory mechanisms are involved in observed cell behavior. A critical role of intracellular Ca^{2+} regulation in cellular stimulation from thermal gradients has been indicated in several cell types. In HeLa cells, thermal rises of only a few tenths degrees, but 1- to 2-s long, have been shown to create a slight uptake of Ca^{2+} by sarco/endoplasmic reticulum Ca^{2+}/ATPase (SERCA) and then an overshoot of cytoplasmic free Ca^{2+} from the ER due to IP_3-channels activation.[24] Additionally, IR-induced intracellular Ca^{2+} transients originating from mitochondrial stores have been shown to be sufficient to modulate the activity of excitable neonatal cardiomyocytes, spiral and vestibular ganglion neurons.[25,26] However, the addition of endoplasmic ryanodine receptors (RyR) blockers significantly reduced IR-induced Ca^{2+} response as well. IR pulses could also produce contraction of cardiomyocytes in the Ca^{2+}-free media and without noticeable Ca^{2+} transients.[27,28] These results suggest that internal Ca^{2+} modulatory mechanisms might dominate over Ca^{2+} influx during IR stimulation.

Recently, we demonstrated that in nonexcitable CHO cells, a ≥3.1-mJ IR pulse exposure initiates the phosphatidylinositol$_{4,5}$-biphosphate (PIP_2) intracellular signaling cascade.[21] This critical physiological regulatory mechanism culminates in

*Address all correspondence to: Gleb P. Tolstykh, E-mail: gleb.tolstykh.ctr@us.af.mil

2329-423X/2017/$25.00 © 2017 SPIE

production of multiple second messengers, including IP_3-dependent intracellular Ca^{2+} release and activation of Ca^{2+}-dependent phospholipase C (PLC) and protein kinase C (PKC).[29–31] Intracellular activity of PKC has been implicated in the modulation of thermo-sensitive TRP channels (TRPV1-4, TRPM8, and TRPA1).[32,33] PIP_2 signaling is also involved in regulation and sensitization of the store-operated TRP channels (SOC),[34–37] some of which are reported to be the core of the mechanosensitive system of mammalian cells.[38–40] Neuronal voltage-gated Ca^{2+} channels (VGCC), SOC, thermo- and mechanosensitive TRP channels all transport Ca^{2+} into the cells and could be responsible for IR-induced intracellular Ca^{2+} increase as an alternative to possible plasma membrane nanoporation.[21] Ca^{2+} also plays multiple roles in cellular physiology, including acting as a charge carrier across the plasma membrane and as a second messenger itself, enabling additional modulatory mechanisms. Thus, it is not surprising that intracellular Ca^{2+} fluctuations are accepted as one of the main hallmarks of neuronal excitability and could be a critical component for understanding the mechanisms of IR-induced neurological stimulation or inhibition.

In this paper, we provide data to progress the fundamental understanding of IR modulation of neurons by revealing the dependence of IR-induced Ca^{2+} mobilization on activation of intracellular Ca^{2+} stores and Ca^{2+} itself, whether from an internal or extracellular origin. By using ratiometric calcium imaging, we obtain quantitative measurements of calcium concentration to limit potential complications of intensity-based calcium indicators in environments with changing baseline cytosolic Ca^{2+} concentrations. Since mitochondrial Ca^{2+} cycling is important in regulation of Ca^{2+} homeostasis of all mammalian cells, we also use the innate difference in Ca^{2+} stores between nonexcitable and excitable (neuron-derived) cell types to compare the sensitivity of IR-induced Ca^{2+} response to these stores. CHO-hM_1, a nonexcitable cell line that lacks VGCCs,[41] and rodent NG108 neuroblastoma, a neuro-derived cell line that does not produce AP in an early undifferentiated state but does contain multiple voltage-gated channels,[42] were used to directly compare the sensitivity of IR-induced Ca^{2+} response without confounding effects from AP.

2 Materials and Methods

2.1 *Cell Culture*

Rodent neuroblastoma-glioma cells (NG108) were grown in Dulbecco's modified Eagle's medium without sodium pyruvate containing 10% fetal bovine serum, 1 I.U./mL penicillin, 0.1 μg/mL streptomycin, 0.1 mM hypoxanthine, 400 nM aminopterin, and 0.016 mM thymidine. Chinese hamster ovarian cells (CHO-hM_1) stably expressing human muscarinic acetylcholine receptor type 1 (hM_1) were grown in F-12K medium containing 10% fetal bovine serum, 1 I.U./mL penicillin, and 0.1 μg/mL streptomycin. Geneticin® (G418) is used in the CHO medium to maintain the hM_1 expressing phenotype. Both cell lines were cultured at 37°C, 5% CO_2, and 95% humidity.

2.2 *Solutions*

Solutions were exchanged through bath application using a Warner Instruments perfusion system at a flow rate of 2 mL/min. Unless otherwise noted, in most experiments, we used a standard external buffer solution (pH 7.4, 290 to 310 mOsm) that consisted of 2 mM magnesium chloride ($MgCl_2$), 5 mM potassium chloride (KCL), 10 mM (4-(2-hydroxyethyl)-1-piperazineethanesulfonic acid) (HEPES), 10 mM glucose, 2 mM calcium chloride ($CaCl_2$), and 135 mM sodium chloride (NaCl). In some experiments (which are noted in the text), the $CaCl_2$ was replaced with 2 mM Na-ethylene glycol-bis(β-aminoethyl ether)-N,N,N′,N′-tetraacetic acid (EGTA) to create Ca^{2+}-free external buffer.

To investigate the sources of IR-induced intracellular Ca^{2+} rises and compare IR effects with well-known effects caused by endogenous PLC activation, some experiments were paired with $G_{q/11}$-coupled hM_1 receptor agonist, oxotremorine (OxoM, 10 μM), $G_{q/11}$-coupled B_1 receptor agonist, bradykinin (BK, 100 nM), or RyR agonist caffeine (10 mM). Additionally, we used IP_3 receptor (IP_3R) blockers xestospongin C (XeC 20 μM), 2-aminoethoxydiphenil borate (2-APB 50 μM), and RyR blocker ryanodine (10 μM). Media, chemicals, and pharmaceuticals were obtained from Life Technologies, Tocris Bioscience, or Sigma-Aldrich. In initial experiments, propidium iodide (PI) (BD Bioscience) was added to the external solution to a concentration of 4 μM to verify cell viability[43] and safe IR fiber placement.

2.3 *Infrared Laser Stimulation*

An Acculight Capella IR diode laser (Lockheed Martin) with a center wavelength of 1869 nm was used to stimulate the cells. As demonstrated in Fig. 1(a), the laser light was delivered to the sample by a 200-μm core optical fiber. A 90-μm region in the center of the fluorescent image was used to analyze the Ca^{2+} response, to ensure uniformity of exposure [Fig. 1(b), green circle]. The fiber tip (top edge) was positioned by a micromanipulator about 90 μm away from the center to avoid obstruction of the region of interest by the fiber. The laser pulse was synchronized with the microscope using the Olympus real-time controller. The rapid rise temperature during stimulation caused intensity fluctuations in the images, possibly from thermal lensing. This "spiking" artifact effect was manually removed from data sets for clear presentation of IR-induced intracellular Ca^{2+} changes.

All IR stimulation experiments were performed with the laser set to deliver 5 pulses (a 1-s, 5-Hz pulse train) with individual pulse durations from 2 (2.5 mJ) to 3 ms (3.8 mJ). Pulse energy was determined at the fiber and the absorption of water was not

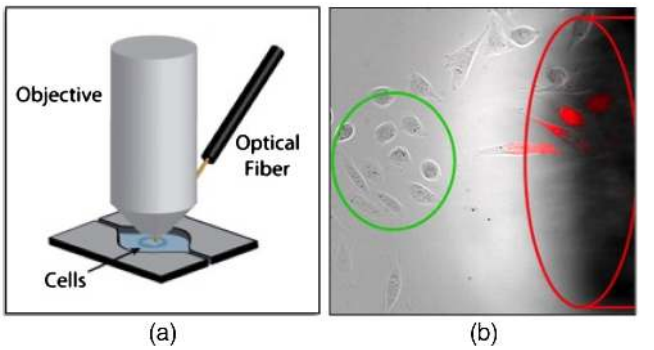

Fig. 1 (a) Diagram showing the position of the IR fiber in relation to the sample and (b) actual image of the cells and optical fiber. Cells in the green circle were used for measurements. The delivery fiber is outlined in red. PI is shown as the red fluorescence signal overlay. (From Olsovsky et al.[46])

taken into account. To ensure that the IR laser pulse was not acutely damaging the cells, uptake of PI was monitored after IR pulse exposure. Uptake of PI can indicate damage to the plasma membrane and PI was seen in cells were directly beneath and in front of the fiber where the temperature rises were significantly higher [Fig. 1(b)]. Thus, the cells that were used for experiments [Fig. 1(b), green circle] were selected from a region that did not demonstrate any PI uptake after many minutes after the IR exposure.

2.4 *Measurement of Calcium*

Cells were plated on poly-L-lysine coated glass coverslips and kept in a 37°C, humidified (5% CO_2) incubator for 24 to 48 h before imaging. The cells were then loaded with Fura-2 Ca^{2+} probe in a standard external buffer solution containing 5 μM Fura-2 and 0.05% pluronic acid at 20°C for 30 min. The dye solution was then replaced with standard outside buffer solution for at least 15 min before imaging.

Fluorescent images were recorded using an Olympus epi-fluorescence microscope with a Lambda DG arc lamp and filter, a Hamamatsu Orca Flash 4.0 sCMOS camera, and an Olympus real-time controller. The real-time controller synchronizes the Lambda filter and camera so that an image using 340-nm excitation wavelength is captured immediately before another image using 380-nm excitation wavelength. The two images are compiled into a ratiometric image. The measured background and average autofluorescence for each cell line were subtracted before calculating the ratio. This ratio correlates to the concentration of calcium and is less vulnerable to artifact caused by variations in intensity due to, for example, defocus or sample thickness. The ratios were converted to Ca^{2+} concentrations using the following equation:

$$[Ca^{2+}]_{free} = \beta \times K_d \times \frac{R - R_{min}}{R_{max} - R},$$

where R is the measured ratio from the image and K_d is the dissociation constant of Fura-2 as reported by Grynkiewicz et al.[44] R_{min}, R_{max}, and β are the minimum ratio, maximum ratio, and scaling factor, respectively, obtained by using Fura-2 calibration kit from Invitrogen. The calibration kit samples were pH 7.2, ionic strength 100 mM KCl, and 50 μM Fura-2. R_{min} is the measured ratio from the images of the sample containing 0 μM free calcium and R_{max} is the ratio from the images of the sample containing 39 μM free Ca^{2+} (beyond saturation of Fura-2). β is the fluorescence using 380-nm excitation on the 0 μM free Ca^{2+} sample over the fluorescence from the 39 μM free Ca^{2+} sample. The final values used in our experiments for K_d, R_{min}, R_{max}, and β were 224 nM, 0.207, 7.18, and 7.5, respectively.

3 Results and Discussion

3.1 *Intracellular Ca^{2+} After Infrared Exposure*

The resulting traces for the intracellular Ca^{2+} concentration increase after IR pulse exposures are shown in Fig. 2. A train of five IR pulses of 2, 2.5, or 3 ms duration started 660 ms after the beginning of image acquisition and lasted for 800 ms. In the Ca^{2+}-containing standard outside buffer solution, noticeable intracellular Ca^{2+} increases appeared during IR pulses and peaked 260 ms after the train in both NG108 and CHO-hM_1. Ca^{2+} rise began immediately after the first

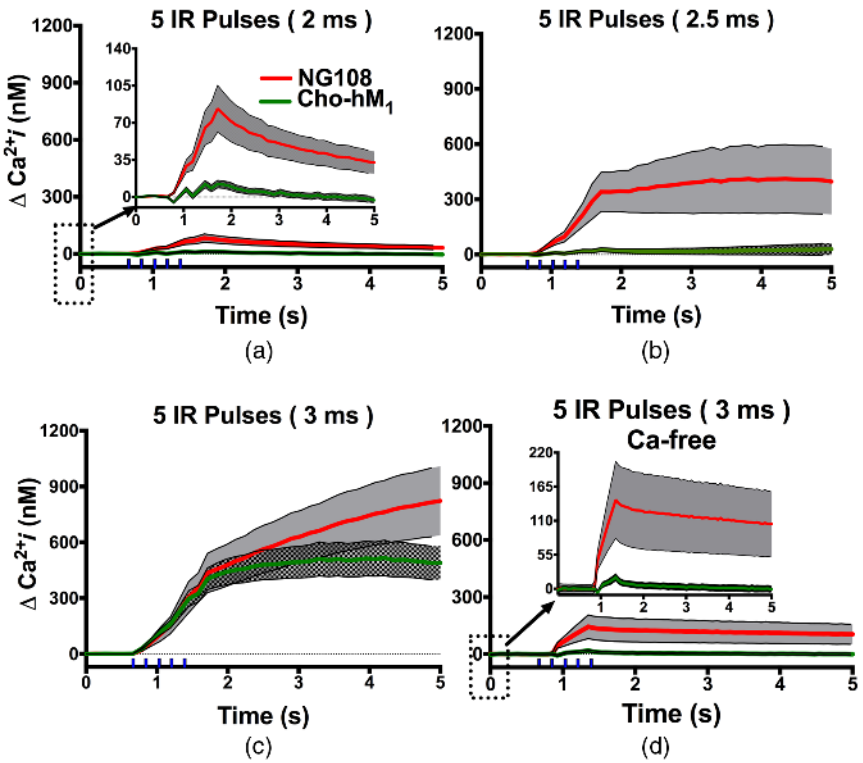

Fig. 2 Comparison of intracellular Ca^{2+} increases after train of IR pulses of different duration between NG108 and CHO-hM_1 cell lines. (a–c) Exposures were performed in Ca^{2+} containing extracellular media. (d) Experiments performed in Ca^{2+} chelated outside media. Error bars (gray area) represent the standard error (SE) of the mean of 5 to 32 cells per group. Vertical ticks above *x*-axis indicate the IR pulses train.

IR pulse and increased with each subsequent pulse and has previously been shown to be evoked by each laser pulse.[45] The mean amplitudes at the peak of intracellular Ca^{2+} after 2 and 2.5 ms IR trains were significantly lower in CHO-hM_1 than in NG108 [Figs. 2(a) and 2(b)]. The delta changes were 12.3 ± 3.7 nM ($n = 20$) versus 83.3 ± 21.1 nM ($n = 9$) for 2 ms IR pulse trials and 26.4 ± 11.4 nM ($n = 20$) versus 340.8 ± 106.8 ($n = 5$) for 2.5 ms pulses for CHO-hM_1 versus NG108, respectively ($p \leq 0.0001$, unpaired two-tailed t-test). For the longer pulses [Fig. 2(c), 3 ms, 3.8 mJ], the intracellular Ca^{2+} increases were much higher than at lower IR pulses amplitudes, but increases observed between CHO-hM_1 and NG108 become statistically insignificant (403.1 ± 58 nM, $n = 32$ versus 435.19 ± 105.4 nM, $n = 19$, respectively, $p \leq 0.77$). Additionally, intracellular Ca^{2+} rise reaches a plateau 1.5 s after the end of the pulse train in CHO-hM1 but continues to rise in NG108 exposed cells. We then compared the increase in intracellular Ca^{2+} after a train of 3 ms pulses in Ca^{2+}-chelated extracellular media [Fig. 2(d)]. We found these intracellular Ca^{2+} concentration increases to be much smaller than in experiments with Ca^{2+}-containing external solution (postexposure $\Delta Ca^{2+}i$ 18.4 ± 5.7 nM, $n = 21$ for CHO-hM_1 and 146.2 ± 59.4 nM, $n = 18$ for NG108), but still determined significant.

From our previous work suggesting that Ca^{2+} rises from IR pulse exposure were due to Ca^{2+} influx from extracellular media,[21,46] we hypothesized that the exposure may create small pores in the plasma membrane. However, the presence of an intracellular Ca^{2+} rise in the absence of external Ca^{2+} suggests that Ca^{2+} increases after IR exposure is not the result of simple passive diffusion through a permeabilized plasma membrane, but rather, a complex and regulated process, possibly through the involvement of IP_3-sensitive endoplasmic reticulum (ER) stores and Ca^{2+}-induced-Ca^{2+}-release (CICR) from ryanodine-sensitive Ca^{2+} stores. Additionally, in both Ca^{2+}-containing and Ca^{2+}-chelated solution, CHO-hM_1 did not exhibit as high a Ca^{2+} increase as NG108. The composition and distribution of plasma membrane ion channels responsible for normal cellular homeostasis and function are markedly different between mammalian excitable and nonexcitable cells. Similar differences are also present in the membranes of major intracellular Ca^{2+} stores. For example, muscular, neuronal, and cardiomyocyte cells widely express both RyR and IP_3R in the sarco-ER, but nonexcitable cells express mostly intracellular IP_3R.[47] The differences in expression in the ER of RyR and IP_3R in excitable and nonexcitable cells could be one of the main regulatory mechanisms responsible for the sensitivity of these cells to external stressors, such as IR stimulation.

Furthermore, the Ca^{2+} rise can be blocked in IR-exposed NG108 and CHO-hM_1 in Ca^{2+}-chelated external media supplemented with thapsigargin.[46] Thapsigargin blocks SERCA, which normally pumps Ca^{2+} from the cytosol into the lumen of the sarco-ER,[48–50] thereby resulting in the depletion of intracellular stores. Remaining Ca^{2+} is eventually cleared by plasma membrane Ca^{2+} pumps.[51] Thus, the lack of a Ca^{2+} increase after IR stimulation seen in these depleted cells suggests that increase in Ca^{2+}-free solution may originate from ER or ryanodine-sensitive Ca^{2+} stores.

3.2 *Role of Intracellular Ca^{2+} Stores in Ca^{2+} Rises After Infrared Exposure*

To investigate the role that these Ca^{2+} stores may be playing in the INM response, we then performed a series of experiments with agonists of the RyR and IP_3R in NG108 and CHO-hM_1. First, to demonstrate the functional expression of intracellular ER receptors and capability of NG108 to adjust to changes in extracellular Ca^{2+}, a series of solution changes were conducted during Ca^{2+} imaging (Fig. 3). NG108 were bathed in

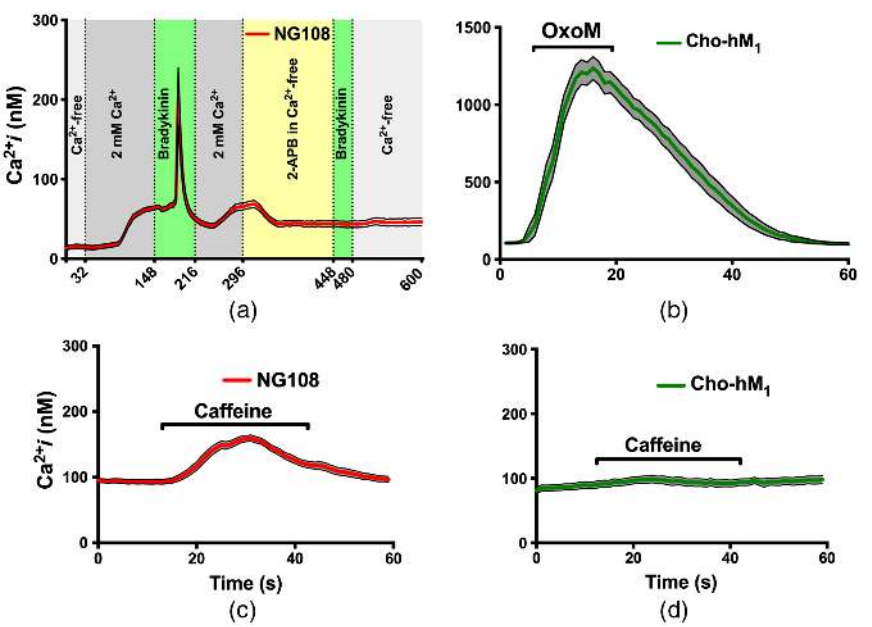

Fig. 3 Intracellular RyR and IP_3Rs in the NG108 and CHO-hM_1 cells. (a) Demonstration of the NG108 cells ($n = 9$) capability to adjust to changes in extracellular Ca^{2+} concentration and respond to 100 nM BK-induced IP_3Rs activation. (b) OxoM (10 μM)-induced intracellular Ca^{2+} rise in CHO-hM_1 cells ($n = 15$) due to ER IP_3Rs activation. (c) Caffeine (10 mM)-induced Ca^{2+} increase due to intracellular RyR receptors activation in the NG108 cells ($n = 17$). (d) Lack of response to 10 mM caffeine in CHO-hM1 cells ($n = 18$). Error bars (black outline with gray area fill) represent the SE of the mean.

Ca^{2+}-chelated buffer for 30 min before beginning ratiometric Ca^{2+} imaging to partially deplete intracellular Ca^{2+} out of the unstimulated cells.[52] The normal resting intracellular Ca^{2+} concentration is between 50 and 100 nM,[53,54] but this exposure depleted it to 15 ± 3 nM [Fig 3(a)]. Shortly after beginning perfusion of cells with Ca^{2+}-containing solution, the resting intracellular Ca^{2+} concentration reached a normal 52 ± 3 nM due to a capacitive Ca^{2+} entry mechanism. Treatment of NG108 with 100 nM BK peptide caused activation of the $G_{q/11}$-coupled B_1 receptors, consequentially initiating PIP_2 signaling and production of the IP_3. After the IP_3-induced Ca^{2+} spike, we applied 2-APB (50 μM) in Ca^{2+}-chelated buffer to block IP_3R and slightly deplete intracellular Ca^{2+} stores.[55] This manipulation prevented the IP_3-induced Ca^{2+} spike after secondary application of the BK and confirmed the functional role of IP_3R in NG108. Similarly, CHO-hM_1 stably expresses the $G_{q/11}$-coupled hM_1 receptors, so application of a high concentration of hM_1 agonist OxoM (10 μM) resulted in a strong IP_3-dependent Ca^{2+} response [Fig. 3(b)].[29] To demonstrate CICR from ryanodine stores, we applied caffeine (10 mM) to sensitize RyR and allowed basal cytosolic calcium levels to actuate CICR.[56,57] A cytoplasmic Ca^{2+} rise can be seen in the NG108, but CHO-hM_1, which do not contain ryanodine stores, shows no response [Figs. 3(c) and 3(d)].

To investigate the role of RyR and IP_3R in the IR-induced changes in intracellular Ca^{2+} dynamics, we exposed both NG108 and CHO-hM_1 to a 3-ms IR pulses train in the presence of several receptor antagonists. Antagonists of RyR and IP_3R dramatically reduced IR-induced intracellular Ca^{2+} response in both cell lines [Fig. 4(a)], suggesting that physiological Ca^{2+} regulatory mechanisms are predominate in the cellular response to IR stimulation.

The IP_3 stores, as shown above (Fig. 4), are present in both NG108 and CHO-hM_1. We pretreated CHO-hM_1 cells for 20 min with XeC (20 μM), a specific inhibitor of the IP_3-dependent Ca^{2+} release.[58] In CHO-hM_1, XeC nearly completely blocked the rise in intracellular Ca^{2+} levels (postexposure $\Delta\,Ca^{2+}i\ 3.3 \pm 0.5$ nM, $n = 13$), even in Ca^{2+}-containing outside buffer. Despite the fact that such a small response is within normal intracellular Ca^{2+} physiological fluctuations, the rise correlates temporally with IR exposure [Fig. 4(b)]. This small increase could be due to capacitive entry of extracellular Ca^{2+} through diacylglycerol (DAG)-sensitive TRP/SOC channels or from incomplete block of the IP_3R.[34,35,59,60] In NG108, a similar small intracellular Ca^{2+} response could lead to CICR from RyR Ca^{2+} stores. Indeed, IR stimulation of NG108 cells in Ca^{2+}-chelated outside buffer and treated with XeC (20 μM) resulted in a small, but significant Ca^{2+} rise (postexposure $\Delta\,Ca^{2+}i\ 38.2 \pm 6.4$ nM, $n = 11$). Additionally, NG108 pretreated with RyR antagonist ryanodine[61] (10 μM) in Ca^{2+}-containing buffer, showed a large reduction in Ca^{2+} rise after IR stimulation (postexposure $\Delta\,Ca^{2+}i\ 16.1 \pm 6.2$ nM, $n = 16$), with the small rise in Ca^{2+} possibly resulting from IP_3 stores or capacitive entry[37,40] without CICR [Fig. 4(b)]. These results show that IP_3 stores are involved in Ca^{2+} signaling from INM in both cell lines but are not the sole Ca^{2+} source in NG108.

Our observations further suggest that differences between excitable and nonexcitable cells in IR-induced Ca^{2+} responses could be due to distinct expression of intracellular RyR and IP_3R in the ER of these cells. RyR and IP_3R have been shown to be activated in parallel with store-operated Ca^{2+} entry (SOCE) and strongly contribute to the global Ca^{2+} response.[62] Depletion of these intracellular Ca^{2+} stores can initiate SOCE through plasma membrane SOC channels. Thus, much of the observed Ca^{2+} increase in the NG108 could be due to direct or indirect activation of RyR and additional to SOCE intracellular Ca^{2+} regulatory mechanism. In NG108, it has been demonstrated that depolarization-induced Ca^{2+} entry evoked CICR only from the ryanodine-sensitive stores,[63] which greatly contribute to general Ca^{2+} response.

Previous experiments on HeLa cells, cardiomyocytes, and neurons have demonstrated the critical role of intracellular Ca^{2+} regulation in thermal gradient stimulation mechanisms. In HeLa cells, during second-long heating of <1 deg, a decrease in Ca^{2+} was observed, theorized to be due to an increase of SERCA activity along with a decrease in the open probability of the ER IP_3R and RyR. After the exposure, the rapid cooling was hypothesized to increase the open probability of these ER Ca^{2+} conducting channels, leading to an overshoot of cytoplasmic Ca^{2+}. This IR-induced Ca^{2+} uptake by SERCAs and its asymmetrical outflow via intracellular ER IP_3R were proposed as a general mechanism of the temperature-dependent changes in Ca^{2+} dynamics.[24] While we did not observe a decrease in Ca^{2+} in these experiments, due to the brevity of our pulses and experimental parameters, this hypothesized sensitivity of the ER IP_3R could contributed the Ca^{2+} overshoot observed

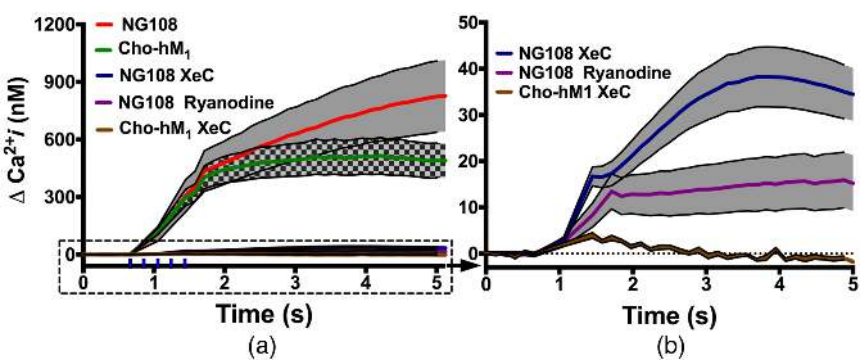

Fig. 4 NG108 and CHO-hM_1 Ca^{2+} responses in Ca^{2+}-containing outside buffer after trains of 3-ms duration IR pulses with and without intracellular RyR and IP_3R blockers. (a) IR-induced changes in intracellular Ca^{2+} dynamics. The traces without antagonists are the same as in Fig. 2 and presented here for comparison. Vertical ticks above *x*-axis indicate the IR pulses train. (b) Magnification of the Ca^{2+} responses with RyR and IP_3R antagonists. Error bars (black outline with gray or black/gray checked pattern fill areas) represent the SE of the mean ($n = 11$ to 16).

from IR pulses. IR rapid heating/cooling of water also creates capacitive photothermal currents, which results in plasma membrane depolarization/repolarization[19] and thus possible activation of the voltage sensitive phosphatase (Ci-VSP). Recently, Ci-VSP was shown to regulate PIP_2 signaling in the plasma membrane[64–66] and could be accounted for the initial depletion during IR-induced cellular response.

Previous IR pulse experiments in cardiomyocytes and spiral and vestibular ganglion neurons indicated that the calcium signaling originated from the mitochondria. However, three (ryanodine, cyclopiazonic acid, and ruthenium red) of the pharmaceutical compounds used in these studies have direct severe inhibitory effect on the RyR and ER, indicating a likely critical importance of internal Ca^{2+} ER pools/receptors in IR-induced INM in addition to alteration of mitochondrial function.[26] By using two cell lines with innate differences in ER receptors, we demonstrate the role that the interplay between these two receptors has on the response the IR exposure.

Previously, we found that IR pulses initiated the intracellular phosphoinositide PIP_2 signaling cascade in CHO-hM_1.[21] This response appeared similar to one initiated by activation of $G_{q/11}$-coupled receptors and resulted in IP_3 production with possible consequential depletion of the intracellular ER Ca^{2+} stores. IP_3 is a main component of the intracellular calcium signaling and provides a direct link between cellular plasma membrane and prime intracellular Ca^{2+} store, the ER.[30,67–70] The exact mechanism of IR-induced activation of PIP_2 signaling is unknown, but hypothetical schematics of the IR-induced Ca^{2+} responses are presented in Fig. 5.

In nonexcitable cells [Fig. 5(a)], IR-induced PLC-dependent PIP_2 hydrolysis or depletion leads to production of IP_3 and DAG (green arrows). DAG and its derivative, arachidonic acid, activate Ca^{2+}-conducting TRP SOC channels[34,35,40,60] and IP_3 initiates intracellular Ca^{2+} release through activation of IP_3R on the ER (blue arrows out of ER). Intracellular Ca^{2+} activates cytoplasmic PKC, which has a high affinity to DAG.[71,72] Active PKC translocates toward DAG (purple arrows) and phosphorylates TRP channels, keeping them in the open state longer.[73] Extracellular Ca^{2+} started to influx into cytosol through TRP/SOC channels due to the SOCE mechanism (red arrows). High levels of intracellular Ca^{2+} catalyze PLC activity, leading to stronger PIP_2 hydrolysis, and potentiating the reaction described above.[29,74] High intracellular Ca^{2+} is eventually pumped out of the cell by plasma membrane Ca^{2+}-ATPase and into ER stores by SERCA.[75,76] In excitable, specifically neuronal cells [Fig. 5(b)], in addition to the reactions described above and SOCE, the intracellular Ca^{2+} increase is achieved through additional mechanisms, including strong sensitization of neurons by IP_3 and Ca^{2+}-activated ryanodine-sensitive Ca^{2+} release.[63,77–79] The interplay of these two intracellular Ca^{2+} pools is critically important, since it leads to much stronger phenotypic Ca^{2+} response. Ca^{2+}- and PIP_2-dependent modulation of the neuronal potassium channels leads to changes in membrane potential and depolarization.[30,80] As a consequence of depolarization and activation of the VGCC, Ca^{2+} influx could also evoke CICR through RyR receptors.[63,79] Last, the overall neuronal activity induces Ca^{2+} influx through excitatory neurotransmitters and receptor-operated Ca^{2+} channels.[81–84] Therefore, IR-induced changes of intracellular Ca^{2+} signaling and dynamics in neurons can explain both stimulation and modulation mechanisms. While additional studies are needed, our experiments presented here indicate that intracellular IP_3R in the ER play an important role in both excitable and nonexcitable cell lines, with the IR-induced Ca^{2+} response augmented by RyR in excitable cells, thus strongly reinforcing our hypothesis.

4 Conclusions

This study directly compared Ca^{2+} mobilization in two very different cells lines, neuronal-like NG108 and epithelial CHO-hM_1, to determine the source of Ca^{2+} rise resulting from INM. As both NG108 and CHO-hM_1 cell models demonstrate an increase in intracellular Ca^{2+} after IR stimulation, the results suggest that Ca^{2+} influx from extracellular space is accompanied by Ca^{2+} derived from the intracellular IP_3 and ryanodine-sensitive Ca^{2+} stores. However, the intracellular Ca^{2+} response in NG108 cells was determined significantly greater, suggesting that interplay of IP_3 and ryanodine intracellular Ca^{2+} pools is critically important to augment the Ca^{2+} rise through CICR after an IR pulsed exposure event.

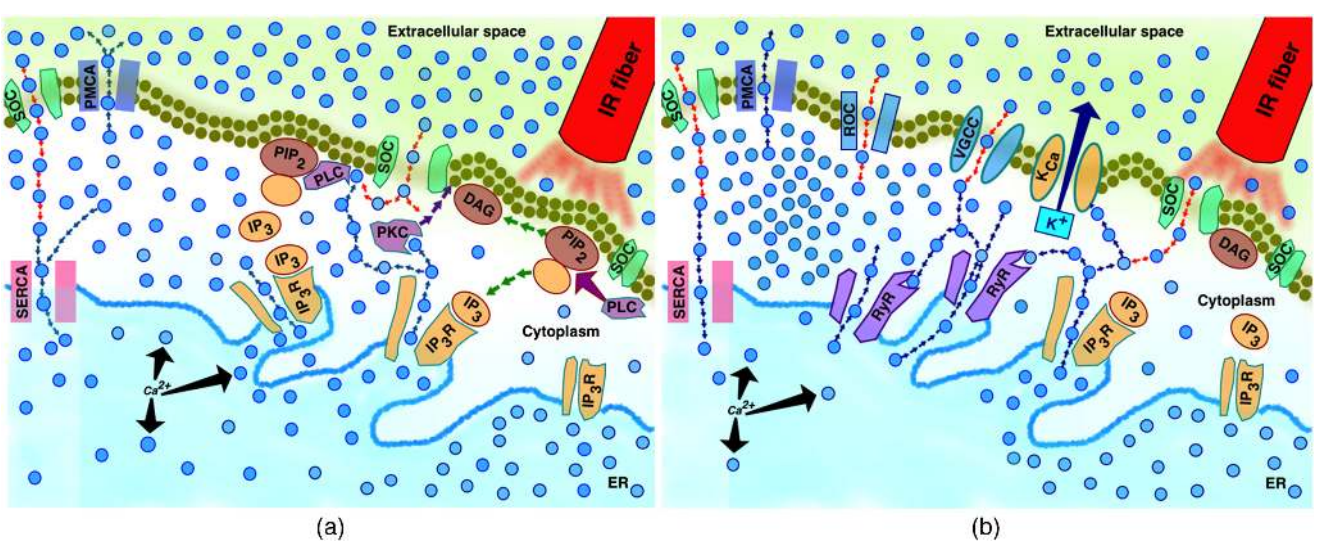

Fig. 5 Simplified hypothetical schematic of IR-induced Ca^{2+} response between (a) nonexcitable and (b) excitable cells.

Disclosures

The authors have no additional relevant financial interests or potential conflicts of interest.

Acknowledgments

This work was supported by the Air Force Office of Scientific Research (LRIR #15RHCOR204). Support for Mr. Cory A. Olsovsky was provided by a Repperger Research Intern Program administered by the Air Force Research Laboratory, 711th Human Performance Wing. CHO-hM_1 cells were donated by Dr. Mark S. Shapiro (University of Texas Health Science Center at San Antonio, Department of Physiology).

References

1. C. P. Richter et al., "Neural stimulation with optical radiation," *Laser Photonics Rev.* **5**(1), 68–80 (2011).
2. C. P. Richter et al., "Spread of cochlear excitation during stimulation with pulsed infrared radiation: inferior colliculus measurements," *J. Neural Eng.* **8**(5), 056006 (2011).
3. I. U. Teudt et al., "Optical stimulation of the facial nerve: a new monitoring technique?" *Laryngoscope* **117**(9), 1641–1647 (2007).
4. J. Wells et al., "Optical stimulation of neural tissue in vivo," *Opt. Lett.* **30**(5), 504–506 (2005).
5. A. I. Matic et al., "Behavioral and electrophysiological responses evoked by chronic infrared neural stimulation of the cochlea," *PLoS One* **8**(3), e58189 (2013).
6. M. Chernov and A. W. Roe, "Infrared neural stimulation: a new stimulation tool for central nervous system applications," *Neurophotonics* **1**(1), 011011 (2014).
7. M. W. Jenkins et al., "Optical pacing of the embryonic heart," *Nat. Photonics* **4**, 623–626 (2010).
8. A. C. Thompson, P. R. Stoddart, and E. D. Jansen, "Optical stimulation of neurons," *Curr. Mol. Imaging* **3**(2), 162–177 (2014).
9. A. J. Walsh et al., "Action potential block in neurons by infrared light," *Neurophotonics* **3**(4), 040501 (2016).
10. A. R. Duke et al., "Spatial and temporal variability in response to hybrid electro-optical stimulation," *J. Neural Eng.* **9**(3), 036003 (2012).
11. A. R. Duke et al., "Transient and selective suppression of neural activity with infrared light," *Sci. Rep.* **3**, 2600 (2013).
12. E. H. Lothet et al., "Alternating current and infrared produce an onset-free reversible nerve block," *Neurophotonics* **1**(1), 011010 (2014).
13. Y. T. Wang, A. M. Rollins, and M. W. Jenkins, "Infrared inhibition of embryonic hearts," *J. Biomed. Opt.* **21**(6), 060505 (2016).
14. N. Kallweit et al., "Optoacoustic effect is responsible for laser-induced cochlear responses," *Sci. Rep.* **6**, 28141 (2016).
15. R. U. Verma et al., "Auditory responses to electric and infrared neural stimulation of the rat cochlear nucleus," *Hear. Res.* **310**, 69–75 (2014).
16. A. C. Thompson et al., "Infrared neural stimulation fails to evoke neural activity in the deaf guinea pig cochlea," *Hear. Res.* **324**, 46–53 (2015).
17. I. U. Teudt et al., "Acoustic events and 'optophonic' cochlear responses induced by pulsed near-infrared laser," *IEEE Trans. Biomed. Eng.* **58**(6), 1648–1655 (2011).
18. J. Wells et al., "Biophysical mechanisms of transient optical stimulation of peripheral nerve," *Biophys. J.* **93**(7), 2567–2580 (2007).
19. Q. Liu et al., "Exciting cell membranes with a blustering heat shock," *Biophys. J.* **106**(8), 1570–1577 (2014).
20. E. S. Albert et al., "TRPV4 channels mediate the infrared laser-evoked response in sensory neurons," *J. Neurophysiol.* **107**(12), 3227–3234 (2012).
21. H. T. Beier et al., "Plasma membrane nanoporation as a possible mechanism behind infrared excitation of cells," *J. Neural Eng.* **11**(6), 066006 (2014).
22. M. G. Shapiro et al., "Infrared light excites cells by changing their electrical capacitance," *Nat. Commun.* **3**, 736 (2012).
23. M. G. Shapiro et al., "Thermal mechanisms of millimeter wave stimulation of excitable cells," *Biophys. J.* **104**(12), 2622–2628 (2013).
24. V. Tseeb et al., "Highly thermosensitive Ca dynamics in a HeLa cell through IP(3) receptors," *HFSP J.* **3**(2), 117–123 (2009).
25. G. M. Dittami et al., "Intracellular calcium transients evoked by pulsed infrared radiation in neonatal cardiomyocytes," *J. Physiol.* **589**(Pt. 6), 1295–1306 (2011).
26. V. Lumbreras et al., "Pulsed infrared radiation excites cultured neonatal spiral and vestibular ganglion neurons by modulating mitochondrial calcium cycling," *J. Neurophysiol.* **112**(6), 1246–1255 (2014).
27. K. Oyama et al., "Microscopic heat pulses induce contraction of cardiomyocytes without calcium transients," *Biochem. Biophys. Res. Commun.* **417**(1), 607–612 (2012).
28. S. A. Shintani et al., "High-frequency sarcomeric auto-oscillations induced by heating in living neonatal cardiomyocytes of the rat," *Biochem. Biophys. Res. Commun.* **457**(2), 165–170 (2015).
29. L. F. Horowitz et al., "Phospholipase C in living cells activation, inhibition, Ca^{2+} requirement, and regulation of M current," *J. Gen. Physiol.* **126**(3), 243–262 (2005).
30. N. Gamper and M. S. Shapiro, "Regulation of ion transport proteins by membrane phosphoinositides," *Nat. Rev. Neurosci.* **8**(12), 921–934 (2007).
31. N. Gamper and M. S. Shapiro, "Target-specific PIP(2) signalling: how might it work?," *J. Physiol.* **582**(Pt. 3), 967–975 (2007).
32. S. Mandadi, P. J. Armati, and B. D. Roufogalis, "Protein kinase C modulation of thermo-sensitive transient receptor potential channels: implications for pain signaling," *J. Natl. Sci. Biol. Med.* **2**(1), 13–25 (2011).
33. S. Mandadi et al., "Activation of protein kinase C reverses capsaicin-induced calcium-dependent desensitization of TRPV1 ion channels," *Cell Calcium* **35**(5), 471–478 (2004).
34. I. Jardin et al., "Phosphatidylinositol 4, 5-bisphosphate enhances store-operated calcium entry through hTRPC6 channel in human platelets," *Biochim. Biophys. Acta* **1783**(1), 84–97 (2008).
35. J. W. Putney, Jr., "Inositol lipids and TRPC channel activation," *Biochem. Soc. Symp.* **74**, 37–45 (2007).
36. M. Trebak et al., "Phospholipase C-coupled receptors and activation of TRPC channels," *Handb. Exp. Pharmacol.* **179**, 593–614 (2007).
37. G. Vazquez et al., "The mammalian TRPC cation channels," *Biochim. Biophys. Acta* **1742**(1–3), 21–36 (2004).
38. P. Gottlieb et al., "Revisiting TRPC1 and TRPC6 mechanosensitivity," *Pflugers Arch.* **455**(6), 1097–1103 (2008).
39. R. Maroto et al., "TRPC1 forms the stretch-activated cation channel in vertebrate cells," *Nat. Cell Biol.* **7**(2), 179–185 (2005).
40. G. M. Salido, S. O. Sage, and J. A. Rosado, "TRPC channels and store-operated Ca^{2+} entry," *Biochim. Biophys. Acta* **1793**(2), 223–230 (2009).
41. N. Gamper, J. D. Stockand, and M. S. Shapiro, "The use of Chinese hamster ovary (CHO) cells in the study of ion channels," *J. Pharmacol. Toxicol. Methods* **51**(3), 177–185 (2005).
42. J. Liu et al., "Voltage-gated sodium channel expression and action potential generation in differentiated NG108-15 cells," *BMC Neurosci.* **13**, 129 (2012).
43. C. C. Roth et al., "Nanosecond pulsed electric field thresholds for nanopore formation in neural cells," *J. Biomed. Opt.* **18**(3), 035005 (2013).
44. G. Grynkiewicz, M. Poenie, and R. Y. Tsien, "A new generation of Ca^{2+} indicators with greatly improved fluorescence properties," *J. Biol. Chem.* **260**(6), 3440–3450 (1985).
45. H. T. Beier et al., "Plasma membrane nanoporation as a possible mechanism behind infrared excitation of cells," *J. Neural Eng.* **11**(6), 066006 (2014).
46. C. A. Olsovsky et al., "Origins of intracellular calcium mobilization evoked by infrared laser stimulation," *Proc. SPIE* **9321**, 93210L (2015).
47. D. L. Bennett et al., "Expression and function of ryanodine receptors in nonexcitable cells," *J. Biol. Chem.* **271**(11), 6356–6362 (1996).
48. G. Inesi et al., "Cell-specific promoter in adenovirus vector for transgenic expression of SERCA1 ATPase in cardiac myocytes," *Am. J. Physiol.* **274**(Pt. 3), C645–C653 (1998).
49. M. S. Kirby et al., "Thapsigargin inhibits contraction and Ca^{2+} transient in cardiac cells by specific inhibition of the sarcoplasmic reticulum Ca^{2+} pump," *J. Biol. Chem.* **267**(18), 12545–12551 (1992).
50. T. B. Rogers et al., "Use of thapsigargin to study Ca^{2+} homeostasis in cardiac cells," *Biosci. Rep.* **15**(5), 341–349 (1995).
51. L. Chen, D. S. Koh, and B. Hille, "Dynamics of calcium clearance in mouse pancreatic beta-cells," *Diabetes* **52**(7), 1723–1731 (2003).
52. R. Chakrabarti and R. Chakrabarti, "Calcium signaling in non-excitable cells: Ca^{2+} release and influx are independent events linked to two

plasma membrane Ca^{2+} entry channels," *J. Cell Biochem.* **99**(6), 1503–1516 (2006).
53. J. Tong, T. V. McCarthy, and D. H. MacLennan, "Measurement of resting cytosolic Ca^{2+} concentrations and Ca^{2+} store size in HEK-293 cells transfected with malignant hyperthermia or central core disease mutant Ca^{2+} release channels," *J. Biol. Chem.* **274**(2), 693–702 (1999).
54. J. L. Nunez and M. M. McCarthy, "Resting intracellular calcium concentration, depolarizing gamma-aminobutyric acid and possible role of local estradiol synthesis in the developing male and female hippocampus," *Neuroscience* **158**(2), 623–634 (2009).
55. T. Maruyama et al., "2APB, 2-aminoethoxydiphenyl borate, a membrane-penetrable modulator of Ins(1, 4, 5)P3-induced Ca^{2+} release," *J. Biochem.* **122**(3), 498–505 (1997).
56. I. Ricard et al., "A caffeine/ryanodine-sensitive Ca^{2+} pool is involved in triggering spontaneous variations of Ca^{2+} in Jurkat T lymphocytes by a Ca(2+)-induced Ca^{2+} release (CICR) mechanism," *Cell Signal* **9**(2), 197–206 (1997).
57. Q. Zhang et al., "R-type Ca(2+)-channel-evoked CICR regulates glucose-induced somatostatin secretion," *Nat. Cell Biol.* **9**(4), 453–460 (2007).
58. J. Gafni et al., "Xestospongins: potent membrane permeable blockers of the inositol 1, 4, 5-trisphosphate receptor," *Neuron* **19**(3), 723–733 (1997).
59. L. Lemonnier, M. Trebak, and J. W. Putney Jr, "Complex regulation of the TRPC3, 6 and 7 channel subfamily by diacylglycerol and phosphatidylinositol-4, 5-bisphosphate," *Cell Calcium* **43**(5), 506–514 (2008).
60. S. Miehe et al., "Inhibition of diacylglycerol-sensitive TRPC channels by synthetic and natural steroids," *PLoS One* **7**(4), e35393 (2012).
61. A. M. Vites and A. J. Pappano, "Distinct modes of inhibition by ruthenium red and ryanodine of calcium-induced calcium release in avian atrium," *J. Pharmacol. Exp. Ther.* **268**(3), 1476–1484 (1994).
62. S. Dadsetan et al., "Store-operated Ca^{2+} influx causes Ca^{2+} release from the intracellular Ca^{2+} channels that is required for T cell activation," *J. Biol. Chem.* **283**(18), 12512–12519 (2008).
63. P. Ronde, J. J. Dougherty, and R. A. Nichols, "Functional IP3- and ryanodine-sensitive calcium stores in presynaptic varicosities of NG108-15 (rodent neuroblastoma x glioma hybrid) cells," *J. Physiol.* **529**(Pt. 2), 307–319 (2000).
64. Y. Murata et al., "Phosphoinositide phosphatase activity coupled to an intrinsic voltage sensor," *Nature* **435**(7046), 1239–1243 (2005).
65. Y. Murata and Y. Okamura, "Depolarization activates the phosphoinositide phosphatase Ci-VSP, as detected in Xenopus oocytes coexpressing sensors of PIP2," *J. Physiol.* **583**(Pt. 3), 875–889 (2007).
66. S. B. Hansen, "Lipid agonism: the PIP2 paradigm of ligand-gated ion channels," *Biochim. Biophys. Acta Mol. Cell Biol. Lipids* **1851**(5), 620–628 (2015).
67. M. J. Berridge, "Inositol trisphosphate and calcium signalling," *Nature* **361**(6410), 315–325 (1993).
68. M. J. Berridge, "Inositol trisphosphate and calcium signalling mechanisms," *Biochim. Biophys. Acta Mol. Cell Biol. Lipids* **1793**(6), 933–940 (2009).
69. M. J. Berridge, P. Lipp, and M. D. Bootman, "The versatility and universality of calcium signalling," *Nat. Rev. Mol. Cell Biol.* **1**(1), 11–21 (2000).
70. E. A. Finch and G. J. Augustine, "Local calcium signalling by inositol-1, 4, 5-trisphosphate in Purkinje cell dendrites," *Nature* **396**(6713), 753–756 (1998).
71. E. Oancea and T. Meyer, "Protein kinase C as a molecular machine for decoding calcium and diacylglycerol signals," *Cell* **95**(3), 307–318 (1998).
72. E. Oancea et al., "Green fluorescent protein (GFP)-tagged cysteine-rich domains from protein kinase C as fluorescent indicators for diacylglycerol signaling in living cells," *J. Cell Biol.* **140**(3), 485–498 (1998).
73. D. C. Immke and N. R. Gavva, "The TRPV1 receptor and nociception," *Semin. Cell Dev. Biol.* **17**(5), 582–591 (2006).
74. G. P. Tolstykh et al., "600 ns pulse electric field-induced phosphatidylinositol-bisphosphate depletion," *Bioelectrochemistry* **100**, 80–87 (2014).
75. M. Seth et al., "Sarco(endo)plasmic reticulum Ca^{2+} ATPase (SERCA) gene silencing and remodeling of the Ca^{2+} signaling mechanism in cardiac myocytes," *Proc. Natl. Acad. Sci. U. S. A.* **101**(47), 16683–16688 (2004).
76. F. Di Leva et al., "The plasma membrane Ca^{2+} ATPase of animal cells: structure, function and regulation," *Arch. Biochem. Biophys.* **476**(1), 65–74 (2008).
77. S. A. Locknar et al., "Calcium-induced calcium release regulates action potential generation in guinea-pig sympathetic neurones," *J. Physiol.* **555**(Pt. 3), 627–635 (2004).
78. J. G. Barbara, "IP3-dependent calcium-induced calcium release mediates bidirectional calcium waves in neurones: functional implications for synaptic plasticity," *Biochim. Biophys. Acta* **1600**(1–2), 12–18 (2002).
79. A. Verkhratsky and A. Shmigol, "Calcium-induced calcium release in neurones," *Cell Calcium* **19**(1), 1–14 (1996).
80. N. Gamper and M. S. Shapiro, "Calmodulin mediates Ca^{2+}-dependent modulation of M-type K+ channels," *J. Gen. Physiol.* **122**(1), 17–31 (2003).
81. L. Antkiewicz-Michaluk, "Receptor and voltage-operated ion channels in the central nervous system," *J. Pharm. Pharmacol.* **47**(3), 253–264 (1995).
82. A. Sanchez-Perez et al., "Modulation of NMDA receptors in the cerebellum. II. Signaling pathways and physiological modulators regulating NMDA receptor function," *Cerebellum* **4**(3), 162–170 (2005).
83. R. Schneggenburger, F. Tempia, and A. Konnerth, "Glutamate- and AMPA-mediated calcium influx through glutamate receptor channels in medial septal neurons," *Neuropharmacology* **32**(11), 1221–1228 (1993).
84. D. M. Simeone, B. C. Kimball, and M. W. Mulholland, "Acetylcholine-induced calcium signaling associated with muscarinic receptor activation in cultured myenteric neurons," *J. Am. Coll. Surg.* **182**(6), 473–481 (1996).

Gleb P. Tolstykh received the Presidential Research Fellowship award in 1995 and completed it at the University of Texas Health Science Center at San Antonio (USA). He continued his research career there, focusing on physiology and neuroscience. He was a Senior National Research Council Fellow (USA) from 2011 to 2013 at the Air Force Research Laboratory (AFRL). Currently, he is a principal scientist at General Dynamics Information Technology, investigating high-energy-induced effects on cellular homeostasis.

Cory A. Olsovsky is a graduate student in the Biomedical Engineering Department at Texas A&M University, College Station, Texas. He received his BS degree in biomedical engineering from Texas A&M University in 2011. His current research is focused on innovative techniques for confocal microscopy.

Bennett L. Ibey received his PhD in biomedical engineering from Texas A&M University in biomedical optics in 2006. He joined AFRL's Radio Frequency Bioeffects Branch in 2007 and serves as a principal investigator for high peak power microwave bioeffects and nanosecond electric pulse research. He is an associate editor for the *Bioelectromagnetics Journal* and a lifetime member of SPIE.

Hope T. Beier has been a research biomedical engineer in AFRL's Optical Radiation Bioeffects Branch since November 2012. She serves as a principal investigator for efforts using advanced optical techniques to investigate the effects of directed energy (laser and radio frequency) on biology. She received her PhD in biomedical engineering from Texas A&M University in 2009. She joined AFRL in 2010 as a National Research Council Postdoctoral Research Associate.